Comparison of Sigma-Ligands and Metabolic PET Tracers for Differentiating Tumor from Inflammation

Aren van Waarde, PhD[1]; Pieter L. Jager, PhD[1]; Kiichi Ishiwata, PhD[2]; Rudi A. Dierckx, PhD[1]; and Philip H. Elsinga, PhD[1]

[1]*Department of Nuclear Medicine and Molecular Imaging, University Medical Center of Groningen, University of Groningen, The Netherlands; and* [2]*Positron Medical Center, Tokyo Metropolitan Institute of Gerontology, Tokyo, Japan*

Novel radiopharmaceuticals for the detection of tumors and their metastases may be of clinical interest if they are more tumor selective than ^{18}F-FDG. Increased glucose metabolism of inflammatory tissues is the main source of false-positive ^{18}F-FDG PET findings in oncology. **Methods:** We compared the biodistribution of 4 PET tracers (2 σ-receptor ligands, ^{11}C-choline, and ^{11}C-methionine) with previously published biodistribution data of 3′-deoxy-3′-^{18}F-fluorothymidine (^{18}F-FLT) and of ^{18}F-FDG in the same animal model. The model consisted of male Wistar rats that bore tumors (C6 rat glioma in the right shoulder) and also had sterile inflammation in the left calf muscle (induced by injection of 0.1 mL of turpentine). Twenty-four hours after turpentine injection, the rats received an intravenous bolus of PET tracer (approximately 30 MBq in the case of ^{18}F and 74 MBq for ^{11}C). **Results:** ^{18}F-FDG showed the highest tumor-to-muscle ratio of all radiopharmaceuticals (13.2 ± 3.0, mean ± SD), followed at a large distance by the σ-1 ligand ^{11}C-SA4503 (5.1 ± 1.7), ^{18}F-FLT (3.8 ± 1.3), the non–subtype-selective σ-ligand ^{18}F-FE-SA5845 (3.3 ± 1.5), ^{11}C-choline (3.1 ± 0.4), and ^{11}C-methionine (2.8 ± 0.3). σ-Ligands and ^{18}F-FLT were relatively tumor selective (^{18}F-FE-SA5845, greater than 30-fold; ^{11}C-SA4503 and ^{18}F-FLT, greater than 10-fold). The tumor selectivity of ^{11}C-methionine was only slightly better than that of ^{18}F-FDG. ^{11}C-Choline showed equal uptake in tumor and inflammation. All tracers were avidly taken up by proliferative tissue (small intestine, bone marrow). High physiologic uptake of some compounds was observed in brain, heart, lung, pancreas, spleen, and salivary gland. **Conclusion:** σ-Ligands and ^{18}F-FLT were more tumor selective than ^{18}F-FDG, ^{11}C-choline, or ^{11}C-methionine in our animal model. However, these novel radiopharmaceuticals were less sensitive than were the established oncologic tracers.

Key Words: tumor; sigma-ligands; inflammation; choline; methionine

J Nucl Med 2006; 47:150–154

Novel radiopharmaceuticals for the visualization of tumors and their metastases may be of clinical interest if they are more tumor selective than ^{18}F-FDG. Increased glucose metabolism of inflammatory tissues is the main source of false-positive PET findings in oncology (*1–3*). Tumor-invading macrophages can induce high ^{18}F-FDG uptake after anticancer therapy (*3–5*).

Various other approaches for tumor visualization have been described in the literature, including the use of radiolabeled amino acids (*1,6,7*), nucleosides (*8–10*), choline (*11–13*), and various receptor ligands (*14–16*). Some of these tracers may show greater tumor selectivity than ^{18}F-FDG. Thymidine and methionine have been reported to show considerable uptake in malignant tissue but much less uptake in inflammatory cells than ^{18}F-FDG (*7,9*). ^{11}C-labeled choline has also been claimed to be better than ^{18}F-FDG for discrimination between proliferative tissue and inflammation (*17*).

In recent years, σ-receptor ligands have been proposed as radiotracers for tumor imaging. Interest in these binding sites was roused for 3 reasons: First, σ-receptors are strongly overexpressed in a large variety of human tumors (*18–20*). Second, the σ-2 receptor density of tumors is a biomarker of cellular proliferation (*21–23*). Third, the activation of intracellular σ-2 receptors increases cytosolic calcium and introduces apoptosis via a caspase- and p53-independent mechanism (*24–26*). A radioligand for visualization of σ-receptors with PET could therefore be useful for detection of primary tumors and their metastases, for noninvasive assessment of tumor proliferative status, and for determination of the σ-receptor occupancy of antineoplastic drugs.

To the best of our knowledge, no information is available about the capability of radiolabeled σ-receptor ligands to differentiate malignant from inflammatory cells. Recently, we developed a rodent model in which each animal bears a tumor and also has sterile inflammation (*27*). This model allows assessment of the tumor selectivity of radiopharmaceuticals, each animal serving as its own control. When we started this project, suitable PET radioligands selective for the σ-2 subtype were not yet available, although a few potential tracers were later described (*28*). Thus, we decided to compare the biodistribution of 2 well-characterized

Received Aug. 31, 2005; revision accepted Oct. 7, 2005.

For correspondence or reprints contact: Aren van Waarde, PhD, Department of Nuclear Medicine and Molecular Imaging, University Medical Center of Groningen, P.O. Box 30001, 9700RB Groningen, The Netherlands.
E-mail: a.van.waarde@pet.umcg.nl

σ-ligands, ^{11}C-SA4503 (selective for the σ-1 subtype) and ^{18}F-FE-SA5845 (not selective for a subtype) (*29*), in this model with that of 4 oncologic PET tracers, namely ^{11}C-choline, ^{11}C-methionine, 3′-deoxy-3′-^{18}F-fluorothymidine (^{18}F-FLT), and ^{18}F-FDG. Data for the last 2 tracers came from a previous publication (*27*). Although a period of 120 rather than 60 min was chosen for sacrificing the animals in the previous report, the data can be compared with those in the present paper because the biodistribution of ^{18}F-FDG and ^{18}F-FLT reaches a steady state between 60 and 120 min.

MATERIALS AND METHODS

Materials

^{18}F-FE-SA5845 and ^{11}C-SA4503 were made by reaction of ^{18}F-fluoroethyl tosylate and ^{11}C-methyl iodide, respectively, with the corresponding 4-*O*-methyl compound (36). The decay-corrected radiochemical yields of ^{18}F-FE-SA5485 and ^{11}C-SA4503 were 4%–7% and 9%–11%, respectively. The specific radioactivities of ^{18}F-FE-SA5485 and ^{11}C-SA4503 were greater than 74 TBq/mmol and greater than 11 TBq/mmol, respectively, at the time of injection. The injected mass of the σ-receptor ligands (a maximum of 6.7 nmol of ^{11}C-SA4503 in a 331-g rat, i.e., 20 pmol/g, and a maximum of 0.5 nmol of ^{18}F-FE-SA5845 in a 331-g rat, i.e., 1.5 pmol/g) did not exceed the tumor-tissue σ-receptor capacity, which has been reported as 98 pmol/g for the σ-1 subtype and 551 pmol/g for the σ-2 subtype in C6 glioma (assuming a cellular protein content of 10%) (*20*). In previous animal studies using the same dose of the ligands, we consistently observed specific binding of ^{11}C-SA4503 and ^{18}F-FE-SA5845 in all target organs, including the C6 tumor (*29*). ^{11}C-Methionine was prepared by methylation of L-homocysteine thiolactone with ^{11}C-methyl iodide. The radiochemical yield was 60%, and specific activities were greater than 2 TBq/mmol. ^{11}C-Choline was synthesized by the reaction of ^{11}C-methyl iodide with dimethylaminoethanol at 100°C for 5 min. Unreacted substrates were removed by evaporation, and ^{11}C-choline was further purified using a cation-exchange resin. The product was dissolved in saline. All radiochemical purities were greater than 95%.

Animal Model

Relevant details about our animal model (including PET images and findings from histology) were reported in a previous paper (*27*). C6 glioma cells (2×10^6, in a mixture of Matrigel [Becton Dickenson] and Dulbecco's minimal essential medium with 5% fetal calf serum) were subcutaneously injected into the right shoulder of male Wistar rats, 11 d before tracer injection. Ten days later, 0.1 mL of turpentine was intramuscularly injected into the thigh of the left hind leg, to produce a sterile inflammation within 24 h. Turpentine injection is an established model of sterile inflammation (*27,30*). The animal experiments were performed by licensed investigators in compliance with the Law on Animal Experiments of The Netherlands. Twenty animals were used in total.

Biodistribution Experiments

Eleven days after the inoculation of C6 tumor cells and 24 h after the turpentine injection, the rats were anesthetized using sodium pentobarbital (60 mg/kg intraperitoneally). We used pentobarbital rather than ketamine because ketamine (particularly the *R*-enantiomer) binds to σ-receptors and reduces the target-to-nontarget ratios of σ-ligands (*29*). The animals were kept under anesthesia for the rest of the experiment. A bolus of either ^{11}C-choline, ^{11}C-methionine, ^{11}C-SA4503, or ^{18}F-FE-SA5845 was administered by intravenous injection through a lateral tail vein (0.3 mL containing approximately 74 MBq of the ^{11}C-tracers or 30 MBq of ^{18}F-FE-SA5845). The rats were sacrificed 60 min after radiotracer injection by extirpation of the heart. Blood was collected, and normal tissues (brain, fat, bone, heart, intestines, kidney, liver, lung, skeletal muscle, pancreas, spleen, submandibular gland, and urinary bladder) were excised. Urine was collected, and blood plasma and a blood cell fraction were obtained from blood centrifugation (5 min at 1,000*g*). The complete tumor (1.8 ± 1.0 g) was excised and separated from muscle and skin. Inflamed muscle could be distinguished from the surrounding tissue by its pale color and the odor of turpentine. The inflamed region was excised from the affected thigh. All samples were weighed, and the radioactivity was measured using a CompuGamma CS 1282 counter (LKB-Wallac), applying a decay correction. The results were expressed as dimensionless standardized uptake values (SUVs) (dpm measured per gram of tissue/dpm injected per gram of body weight). Tissue-to-plasma and tumor-to-muscle concentration ratios of radioactivity were also calculated.

Statistical Analysis

Differences between the various tracers were tested for statistical significance using the 2-sided Student *t* test for independent samples. *P* values less than 0.05 were considered significant. Tumor-to-plasma, tumor-to-muscle, and tumor-to-inflammation ratios of tracer uptake were calculated for each rat. A tumor selectivity index was calculated for each tracer and individual animal, using the following formula: (tumor SUV – muscle SUV)/(inflammation SUV – muscle SUV). This figure represents the tumor-to-inflammation ratio corrected for background activity.

RESULTS

Animal Growth and Development of Tumor

The growth rate of a C6 tumor in rats was variable, as reported previously (*27*). Tumor mass at radiotracer injection was 1.8 ± 1.0 g in the present study (mean ± SD; range, 0.29–3.32 g). During the 2 wk of acclimation after purchase and the 11 d after tumor inoculation, the animals showed significant weight gain (about 80 g). Body weight of the rats at the biodistribution experiments was 331 ± 34 g. The animals were fed ad libitum, using standard laboratory chow.

Histologic examination of the excised specimens of tumor and inflamed muscle showed small areas of necrosis in both tissues, composing less than 10% of the total tissue volume.

Biodistribution of ^{11}C-SA4503

Uptake of radioactivity after injection of ^{11}C-SA4503, the radioligand selective for the σ-1 subtype, was highest in the liver, followed by pancreas, kidney, bone marrow, and small intestine. Moderate tracer uptake was found in spleen, submandibular gland, lung, large intestine, brain, and C6 tumor. Low uptake of radioactivity was observed in heart, adipose tissue, muscle, plasma, and red blood cells (Table 1).

TABLE 1
SUVs at 60 Minutes After Injection

Tissue	^{11}C-Choline (n = 4)	^{11}C-Methionine (n = 4)	^{11}C-SA4503 (n = 6)	^{18}F-FE-SA5845 (n = 6)
Cerebellum	0.23 ± 0.05	0.79 ± 0.05	1.08 ± 0.25	0.99 ± 0.24
Cortex	0.23 ± 0.04	0.68 ± 0.09	1.05 ± 0.29	1.08 ± 0.21
Rest of brain	0.21 ± 0.02	0.57 ± 0.08	1.12 ± 0.18	1.06 ± 0.13
Adipose tissue	0.18 ± 0.03	0.09 ± 0.03	0.26 ± 0.12	0.23 ± 0.11
Urinary bladder	1.03 ± 0.28	1.06 ± 0.47	0.62 ± 0.10	0.87 ± 0.37
Bone	0.89 ± 0.20	0.74 ± 0.20	0.40 ± 0.17	0.74 ± 0.13
Bone marrow	2.67 ± 0.87	3.78 ± 0.77	2.31 ± 1.05	1.33 ± 0.12
Heart	2.05 ± 0.19	0.94 ± 0.16	0.24 ± 0.07	0.24 ± 0.05
Large intestine	2.45 ± 0.74	1.23 ± 0.24	1.12 ± 0.19	1.45 ± 0.34
Small intestine	2.57 ± 0.71	2.72 ± 1.02	2.22 ± 0.53	1.67 ± 0.22
Kidney	10.54 ± 1.09	2.54 ± 0.20	3.67 ± 0.93	3.06 ± 0.85
Liver	7.91 ± 1.07	6.12 ± 0.82	7.40 ± 1.63	7.40 ± 1.45
Lung	6.50 ± 0.50	1.45 ± 0.14	1.43 ± 0.35	1.35 ± 0.27
Muscle	0.40 ± 0.04	0.35 ± 0.06	0.15 ± 0.04	0.21 ± 0.06
Pancreas	4.97 ± 0.82	6.40 ± 0.72	4.06 ± 1.70	4.21 ± 0.78
Plasma	0.27 ± 0.03	1.13 ± 0.21	0.07 ± 0.01	0.17 ± 0.03
Red blood cells	0.13 ± 0.02	0.46 ± 0.22	0.05 ± 0.02	0.10 ± 0.04
Spleen	4.31 ± 0.54	2.61 ± 0.25	1.91 ± 0.40	1.81 ± 0.27
Submandibularis	3.43 ± 0.46	1.27 ± 0.13	1.84 ± 0.39	2.13 ± 0.10
C6 tumor	1.22 ± 0.20	0.99 ± 0.14	0.73 ± 0.32	0.62 ± 0.12
Inflammation	1.32 ± 0.39	0.47 ± 0.03	0.20 ± 0.07	0.22 ± 0.13
Urine	1.53 ± 0.55	2.96 ± 2.16	0.93 ± 0.76	4.35 ± 3.40

Bone sample contained marrow; thus, bone uptake of ^{18}F does not reflect defluorination.

Tracer uptake was not significantly higher in the inflamed muscle than in the contralateral healthy tissue. Thus, ^{11}C-SA4503 proved to be fairly tumor selective. A value greater than 10 was calculated for the selectivity index (Fig. 1). ^{11}C-SA4503 had the best tumor-to-plasma ratio (10.2 ± 2.7) and the second best tumor-to-muscle ratio (5.1 ± 1.7) of all studied compounds (Fig. 1).

Biodistribution of ^{18}F-FE-SA5845

The biodistribution of the non–subtype-selective σ-ligand ^{18}F-FE-SA5845 was similar to that of ^{11}C-SA4503, as was reported previously for a different animal model (female nude rats, HSD Ham RNU rnu (*29*)). Uptake of ^{18}F was highest in the liver, followed by pancreas, kidney, and submandibular gland. Moderate tracer uptake was found in spleen, intestines, lung, bone marrow, brain, and C6 tumor. Low levels of radioactivity were detected in heart, adipose tissue, muscle, plasma, and red blood cells (Table 1).

Tracer uptake in the inflamed muscle was virtually equal to that in the contralateral healthy leg (Table 1). ^{18}F-FE-SA5845 showed the highest tumor selectivity of all studied compounds. A value greater than 30 was calculated for the

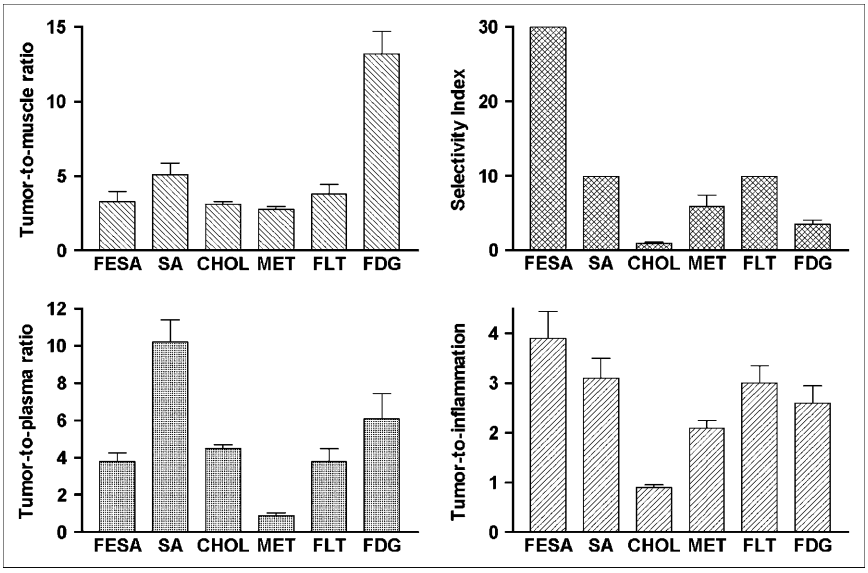

FIGURE 1. Target-to-nontarget ratios and selectivity index (tumor-to-inflammation ratio corrected for background in normal muscle). Data are plotted as mean ± SEM. CHOL = ^{11}C-choline; FESA = ^{18}F-FE-SA5845; MET = ^{11}C-methionine; SA = ^{11}C-SA4503. SEM for selectivity index of FESA, SA, and FLT cannot be given because, in some animals, tracer uptake in inflamed muscle equaled that in contralateral healthy muscle.

selectivity index (Fig. 1). ^{18}F-FE-SA5845 displayed moderate tumor-to-muscle (3.3 ± 1.5) and tumor-to-plasma (3.8 ± 1.0) concentration ratios (Fig. 1).

Biodistribution of ^{11}C-Choline

After injection of ^{11}C-choline, the highest uptake of radioactivity was observed in liver, followed by kidney, lung, pancreas, and spleen. Submandibular gland, bone marrow, intestines, heart, and the C6 tumor showed moderate tracer uptake. Low levels of radioactivity were found in brain, adipose tissue, muscle, plasma, and red blood cells (Table 1).

Quite surprisingly, inflamed muscle accumulated about the same amount of radioactivity as the C6 tumor (Table 1). Thus, ^{11}C-choline did not show any tumor selectivity in this animal model (Fig. 1). Moderate tumor-to-muscle ratios of radioactivity were reached after 1 h, namely 3.1 ± 0.4 (Fig. 1).

Biodistribution of ^{11}C-Methionine

^{11}C-Methionine and ^{11}C-choline had different biodistributions. For ^{11}C-methionine, the highest uptake of radioactivity was in pancreas, followed by liver and bone marrow. Intestines, spleen, kidney, lung, submandibular gland, heart, and the C6 tumor showed moderate tracer uptake. The fairly high levels of radioactivity in plasma were remarkable. Low levels of radioactivity were found in brain, adipose tissue, muscle, and red blood cells (Table 1).

Accumulation of radioactivity in the inflamed muscle was slightly higher than in muscle of the contralateral healthy leg (Table 1). In contrast to ^{11}C-choline, ^{11}C-methionine was moderately tumor selective. A value of 5.9 with a high SD was calculated for the selectivity index (Fig. 1). This high SD is due to variability of tracer uptake in normal muscle tissue. ^{11}C-Methionine showed the lowest tumor-to-muscle ratios of all studied compounds, namely 2.8 ± 0.3 (Fig. 1).

DISCUSSION

^{11}C-SA4503, the radioligand selective for the σ-1 subtype, produced favorable results in our animal model, although this tracer does not bind to σ-2 receptors, which have been reported to be particularly overexpressed in tumor cells, including C6 rat glioma (*20*). The tumor selectivity of ^{11}C-SA4503 (>10) was significantly greater than that of ^{18}F-FDG (3.5 ± 1.2) or ^{11}C-methionine (5.9 ± 3.1) and comparable to the selectivity of the nucleoside ^{18}F-FLT (Fig. 1) (*27*). Moreover, ^{11}C-SA4503 showed the highest tumor-to-plasma ratio (10.2 ± 2.7) and the second highest tumor-to-muscle ratio (5.1 ± 1.7) of all studied tracers (Fig. 1). These data indicate that ^{11}C-SA4503 should be further evaluated to examine its potential for tumor detection in humans. However, ^{11}C-SA4503 and its analog ^{18}F-FE-SA5845 show high physiologic uptake in the central nervous system. The SUV in this healthy tissue is even higher than in the C6 glioma (Table 1). Thus, a high uptake of σ-ligands in normal brain may preclude their use for the detection of brain tumors. Similar limitations are known for ^{18}F-FDG.

The tumor selectivity of the non–subtype-selective σ-ligand ^{18}F-FE-SA5845 was outstanding, a value greater than 30 being reached after 1 h of biodistribution in our rat model (Fig. 1). However, tumor-to-plasma and tumor-to-muscle ratios of ^{18}F-FE-SA5845 were significantly lower than those of ^{11}C-SA4503 and comparable to those of the nucleoside ^{18}F-FLT (Fig. 1). Although ^{18}F-FE-SA5845 binds to both σ-1 and σ-2 receptors with high affinity—in contrast to ^{11}C-SA4503, which binds only to σ-1 receptors—the ^{18}F compound is cleared less rapidly from plasma than is the ^{11}C-labeled drug (Table 1). Lower tumor-to-plasma ratios of ^{18}F-FE-SA5845 are mainly due to a less rapid disappearance of this radioligand from the circulation.

Although some authors have claimed that a better discrimination between proliferative tissue and inflammation is possible with ^{11}C-choline-PET than with ^{18}F-FDG PET (*17,31*), our animal model indicates that ^{11}C-choline is even less tumor selective than ^{18}F-FDG (selectivity index, 1.0 ± 0.2 vs. 3.5 ± 1.2; $P < 0.01$) (Fig. 1). Data from our rat model are in accordance with recent animal and human studies that have described a strong accumulation of ^{11}C-choline and ^{18}F-fluorocholine in inflamed synovium (*32*), pelvic inflammatory disease (*33*), inflammatory granulation tissue (*34*), and experimental bacterial infections (*35*). The underlying cause of the high uptake of ^{11}C-choline by neutrophils is not clear but may be related to a rapid turnover of membrane phospholipids, which are involved in chemotactic signaling and endocytosis.

The tumor selectivity of ^{11}C-methionine was not significantly better than that of ^{18}F-FDG in our animal model (5.9 ± 3.1 vs. 3.5 ± 1.2; $P = 0.22$) (Fig. 1). This observation is in accordance with literature data indicating that ^{11}C-methionine does accumulate in brain abscesses (*36,37*) or sites of chronic inflammation in Rasmussen encephalitis (*38*). Moreover, ^{11}C-methionine has been reported to show high uptake in experimental *Staphylococcus aureus* infections (*39*). Better discrimination between tumor and inflammation may be possible by using methionine with the label in the carboxyl group rather than the methyl group, because the uptake of ^{11}C-carboxyl amino acids is a better reflection of the local protein synthesis rate (*6*), and the mitotic activity of inflammatory cells at the site of inflammation is negligible.

All studied tracers showed moderate to high accumulation in rapidly dividing tissue (bone marrow in the skeleton, mucosa in the intestines, malignant cells in the tumor), as should be expected from proliferation markers. The strikingly high levels of radioactivity that are observed in plasma after injection of ^{11}C-methionine (Table 1) are due to synthesis of plasma proteins (e.g., albumin) by the liver (*6*).

CONCLUSION

The σ-ligand ^{18}F-FE-SA5845 showed high tumor selectivity in our animal model, whereas the tumor selectivity of the σ-1 agonist ^{11}C-SA4503 was comparable

to that of the nucleoside ^{18}F-FLT. The relatively good capability of the σ-ligands to differentiate tumor from inflammation suggests that these radiopharmaceuticals may be of interest for the detection, using PET, of a residual tumor mass after therapy. However, a high physiologic uptake of σ-ligands within the central nervous system can preclude the use of such tracers for the detection of brain tumors. ^{11}C-Choline did not show any tumor selectivity in our rat model. This tracer may produce false-positive PET results in cancer patients.

REFERENCES

1. Strauss LG. Fluorine-18 deoxyglucose and false-positive results: a major problem in the diagnostics of oncological patients. *Eur J Nucl Med.* 1996; 23:1409–1415.
2. Shreve PD. Focal fluorine-18 fluorodeoxyglucose accumulation in inflammatory pancreatic disease. *Eur J Nucl Med.* 1998;25:259–264.
3. Shreve PD, Anzai Y, Wahl RL. Pitfalls in oncologic diagnosis with FDG PET imaging: physiologic and benign variants. *Radiographics.* 1999;19:61–77.
4. Kubota R, Yamada S, Kubota K, et al. Intratumoral distribution of fluorine-18-fluorodeoxyglucose in vivo: high accumulation in macrophages and granulation tissues studied by microautoradiography. *J Nucl Med.* 1992;33:1972–1980.
5. Kaim AH, Weber B, Kurrer MO, et al. Autoradiographic quantification of ^{18}F-FDG uptake in experimental soft-tissue abscesses in rats. *Radiology.* 2002; 223:446–451.
6. Vaalburg W, Coenen HH, Crouzel C, et al. Amino acids for the measurement of protein synthesis in vivo by PET. *Int J Rad Appl Instrum B.* 1992;19:227–237.
7. Jager PL, Vaalburg W, Pruim J, et al. Radiolabeled amino acids: basic aspects and clinical applications in oncology. *J Nucl Med.* 2001;42:432–445.
8. Shields AF, Grierson JR, Dohmen BM, et al. Imaging proliferation in vivo with [F-18]FLT and positron emission tomography. *Nat Med.* 1998;4:1334–1336.
9. Sugawara Y, Gutowski TD, Fisher SJ, et al. Uptake of positron emission tomography tracers in experimental bacterial infections: a comparative biodistribution study of radiolabeled FDG, thymidine, L-methionine, ^{67}Ga-citrate, and ^{125}I-HSA. *Eur J Nucl Med.* 1999;26:333–341.
10. Been LB, Suurmeijer AJ, Cobben DC, et al. [^{18}F]FLT-PET in oncology: current status and opportunities. *Eur J Nucl Med Mol Imaging.* 2004;31:1659–1672.
11. Shinoura N, Nishijima M, Hara T, et al. Brain tumors: detection with C-11 choline PET. *Radiology.* 1997;202:497–503.
12. Hara T, Kosaka N, Kishi H. PET imaging of prostate cancer using carbon-11 choline. *J Nucl Med.* 1998;39:990–995.
13. De Jong IJ, Pruim J, Elsinga PH, et al. Visualization of prostate cancer with ^{11}C-choline positron emission tomography. *Eur Urol.* 2002;42:18–23.
14. Black KL, Ikezaki K, Toga AW. Imaging of brain tumors using peripheral benzodiazepine receptor ligands. *J Neurosurg.* 1989;71:113–118.
15. Lamberts SW, Bakker WH, Reubi JC, et al. Somatostatin-receptor imaging in the localization of endocrine tumors. *N Engl J Med.* 1990;323:1246–1249.
16. Larson S. Receptors on tumors studied with radionuclide scintigraphy. *J Nucl Med.* 1991;32:1189–1191.
17. Sasaki T. [^{11}C]Choline uptake in regenerating liver after partial hepatectomy or CCl_4-administration. *Nucl Med Biol.* 2004;31:269–275.
18. Bem WT, Thomas GE, Mamone JY, et al. Overexpression of sigma receptors in nonneural human tumors. *Cancer Res.* 1991;51:6558–6562.
19. John CS, Bowen WD, Varma VM, et al. Sigma receptors are expressed in human non-small cell lung carcinoma. *Life Sci.* 1995;56:2385–2392.
20. Vilner BJ, John CS, Bowen WD. Sigma-1 and sigma-2 receptors are expressed in a wide variety of human and rodent tumor cell lines. *Cancer Res.* 1995;55: 408–413.
21. Mach RH, Smith CR, Al Nabulsi I, et al. Sigma 2 receptors as potential biomarkers of proliferation in breast cancer. *Cancer Res.* 1997;57:156–161.
22. Al Nabulsi I, Mach RH, Wang LM, et al. Effect of ploidy, recruitment, environmental factors, and Tamoxifen treatment on the expression of sigma-2 receptors in proliferating and quiescent tumour cells. *Br J Cancer.* 1999;81: 925–933.
23. Wheeler KT, Wang LM, Wallen CA, et al. Sigma-2 receptors as a biomarker of proliferation in solid tumours. *Br J Cancer.* 2000;82:1223–1232.
24. Brent PJ, Pang G, Little G, et al. The sigma receptor ligand, reduced haloperidol, induces apoptosis and increases intracellular-free calcium levels $[Ca^{2+}]_i$ in colon and mammary adenocarcinoma cells. *Biochem Biophys Res Commun.* 1996; 219:219–226.
25. Crawford KW, Bowen WD. Sigma-2 receptor agonists activate a novel apoptotic pathway and potentiate antineoplastic drugs in breast tumor cell lines. *Cancer Res.* 2002;62:313–322.
26. Aydar E, Palmer CP, Djamgoz MBA. Sigma receptors and cancer: possible involvement of ion channels. *Cancer Res.* 2004;64:5029–5035.
27. Van Waarde A, Cobben DC, Suurmeijer AJ, et al. Selectivity of ^{18}F-FLT and ^{18}F-FDG for differentiating tumor from inflammation in a rodent model. *J Nucl Med.* 2004;45:695–700.
28. Tu Z, Dence CS, Ponde DE, et al. Carbon-11 labeled sigma(2) receptor ligands for imaging breast cancer. *Nucl Med Biol.* 2005;32:423–430.
29. Van Waarde A, Buursma AR, Hospers GA, et al. Tumor imaging with two sigma-receptor ligands, ^{18}F-FE-SA5845 and ^{11}C-SA4503: a feasibility study. *J Nucl Med.* 2004;45:1939–1945.
30. Yamada S, Kubota K, Kubota R, et al. High accumulation of fluorine-18-fluorodeoxyglucose in turpentine-induced inflammatory tissue. *J Nucl Med.* 1995;36:1301–1306.
31. Khan N, Oriuchi N, Ninomiya H, et al. Positron emission tomographic imaging with ^{11}C-choline in differential diagnosis of head and neck tumors: comparison with ^{18}F-FDG PET. *Ann Nucl Med.* 2004;18:409–417.
32. Roivainen A, Parkkola R, Yli-Kerttula T, et al. Use of positron emission tomography with methyl-^{11}C-choline and 2-^{18}F-fluoro-2-deoxy-D-glucose in comparison with magnetic resonance imaging for the assessment of inflammatory proliferation of synovium. *Arthritis Rheum.* 2003;48:3077–3084.
33. Torizuka T, Kanno T, Futatsubashi M, et al. Imaging of gynecologic tumors: comparison of ^{11}C-choline PET with ^{18}F-FDG PET. *J Nucl Med.* 2003;44:1051–1056.
34. Tian M, Zhang H, Oriuchi N, et al. Comparison of ^{11}C-choline PET and FDG PET for the differential diagnosis of malignant tumors. *Eur J Nucl Med Mol Imaging.* 2004;31:1064–1072.
35. Wyss MT, Weber B, Honer M, et al. ^{18}F-Choline in experimental soft tissue infection assessed with autoradiography and high-resolution PET. *Eur J Nucl Med Mol Imaging.* 2004;31:312–316.
36. Mineura K, Sasajima T, Kowada M, et al. Indications for differential diagnosis of nontumor central nervous system diseases from tumors: a positron emission tomography study. *J Neuroimaging.* 1997;7:8–15.
37. Tsuyuguchi N, Sunada I, Ohata K, et al. Evaluation of treatment effects in brain abscess with positron emission tomography: comparison of fluorine-18-fluorodeoxyglucose and carbon-11-methionine. *Ann Nucl Med.* 2003;17:47–51.
38. Maeda Y, Oguni H, Saitou Y, et al. Rasmussen syndrome: multifocal spread of inflammation suggested from MRI and PET findings. *Epilepsia.* 2003;44:1118–1121.
39. Tang G, Tang X, Wang M, Luo L, Gan M, Wu H. A uptake comparative study of new F-18 labeled amino acid tracers, FDG and [methyl-C-11]-L-methionine in fibrosarcoma-inoculated tumor and *S-aureus* induced infection [abstract]. *J Nucl Med.* 2004;45(suppl):167P